CrossMark

Comparative Degradation of Alachlor Using Photocatalysis and Photo-Fenton

Margarita Hincapié Pérez · Lina Patricia Vega ·
Henry Zúñiga-Benítez · Gustavo A. Peñuela

Abstract A comparative study about the degradation of alachlor in aqueous solutions under different photocatalytic systems, including TiO_2, TiO_2/H_2O_2, and $TiO_2/Na_2S_2O_8$ heterogeneous photocatalysis, Fe^{2+}/H_2O_2, Fe^{3+}/H_2O_2, and UV radiation, was carried out. In this way, times for alachlor total removal and mineralization followed the order photo-Fenton < photocatalysis with persulfate < photo-Fenton-like < photocatalysis with hydrogen peroxide < photocatalysis with TiO_2. Ferric chloride was used as ferric ion source under Fenton-like reactions. Oxidation with Fe^{2+}/H_2O_2 was faster than treatment with Fe^{3+}/H_2O_2, but under UV irradiation, degradation rates were similar, indicating that $FeCl_3$ could be a good source of ferric ions for alachlor degradation. Reduction of the sample toxicity was much faster in the photo-Fenton process than in TiO_2 process (50% mortality reduction in 180 min compared to around 400 min—Daphnia Pullex assays). In addition, evaluation of the nitrogen and chloride contained in the treated samples confirmed a 100% conversion of the N and Cl content in the pollutant molecule. Finally, some of the degradation by-products for pollutant removal using TiO_2 photocatalysis were identified.

1 Introduction

Alachlor, 2-chloro-2,6-diethyl-N-(methoxymethyl) acetanilide (ALC), is a herbicide used to control grasses and broadleaf weeds in crops such as corn, soybeans, and sorghum. In the USA, it is of the most widely used herbicides. However, currently, alachlor is included in the list of priority substances in European Union Water Framework Directive 2000/60/EC, because it is considered a carcinogen category 3 (Directive 2000/7/EC, 2000). In this way, the Environmental Protection Agency (EPA) has set as target for maximum contaminant level goal (MCLG) in water for human consumption at zero and a maximum contaminant level (MCL) value of 0.002 mg L^{-1} (EPA 2009).

Alachlor has been found in groundwater above the maximum concentration limit (MCL) of 0.002 mg L^{-1} (EPA 2009; Ritter 1990). It has a half-life in soil of 70 days and 30 days in water. More than ten transformation products of its degradation have been found in groundwater, in concentrations ranging from 4 to 570 ng L^{-1}, exceeding the parent compound

M. H. Pérez
Departamento de Ingeniería Ambiental, Facultad de Ingeniería, Universidad de Medellín, Carrera 87 No 30-65, Medellín, Colombia

L. P. Vega · H. Zúñiga-Benítez · G. A. Peñuela
Grupo GDCON, Facultad de Ingeniería, Sede de Investigación Universitaria (SIU), Universidad de Antioquia UdeA, Calle 70 No 52-21, Medellín, Colombia

H. Zúñiga-Benítez (✉)
Departamento de Ingeniería Química, Facultad de Ingeniería, Universidad de Antioquia UdeA, Calle 70 No 52-21, Medellín, Colombia
e-mail: henry.zuniga@udea.edu.co

concentration by at least two-fold. Among those, 2′,6′-diethylaniline is of special interest. This compound is frequently detected as a promutagen and may be transformed by rat liver enzyme preparations to 2,6-diethylnitrosobenzene, which is strongly mutagenic (Potter and Carpenter 1995).

Use of advanced treatments for polluted water is becoming necessary to reduce alachlor concentration levels. In this way, advanced oxidation processes have been successfully used for this purpose. Different authors have evaluated the use of TiO_2 heterogeneous photocatalysis, Fenton and photo-Fenton reactions, ultrasound, and some electrochemical techniques for pollutant removal, reaching relevant extents of ALC degradation. In particular, TiO_2 heterogeneous photocatalysis and Fenton reactions have demonstrated their potential to remove a considerable number of organic pollutants from aqueous matrices (de Luna et al. 2015; Kumar et al. 2017; Potter and Carpenter 1995; Wang et al. 2016).

In the photocatalytic oxidation process with TiO_2, photoexcitation of TiO_2 particles promotes the generation of an electron (e^-_{CB}) from the conduction band, leaving a hole (h^+) in the valence band. Hence, oxidative or reductive processes can occur at or near the surface of the catalyst particles and promote the degradation of organic matter. However, one of the disadvantages of this technology is the eventual recombination of the photo-generated electron-hole pairs, limiting the possibility of organic compound oxidation. In this way, it is known that by adding H_2O_2, it is possible to achieve favorable effects in photocatalytic degradation by means of further $OH^.$ radical generation. Additional $OH^.$ radicals are generated via interaction of H_2O_2 with conduction-band electrons as it is shown by Eq. 1, and with superoxide radicals present in the solution (Eq. 2) (Pichat et al. 1995).

$$H_2O_2 + e^-_{CB} \rightarrow OH^. + OH^- \tag{1}$$

$$H_2O_2 + O_2^{.-} \rightarrow OH^. + OH^- + O_2^. \tag{2}$$
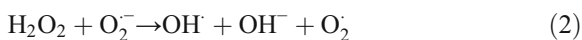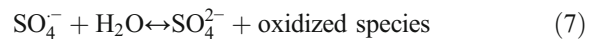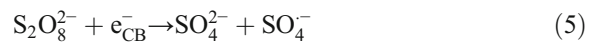
In this sense, additional $OH^.$ radicals could promote a faster degradation and mineralization rates, but, in some cases, hydrogen peroxide may act as scavenger of the photogenerated holes and hydroxyl free radicals according to Eqs. 3 and 4 (Pichat et al. 1995).
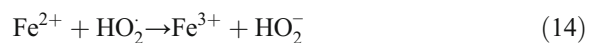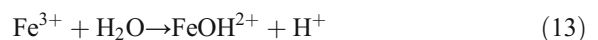
$$H_2O_2 + 2h^+ \rightarrow O_2 + 2H^+ \tag{3}$$

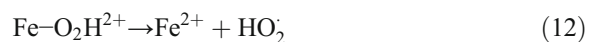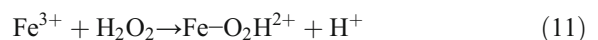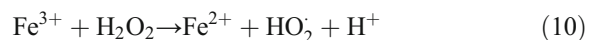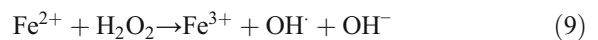$$H_2O_2 + OH^. \rightarrow H_2O + HO_2^. \tag{4}$$
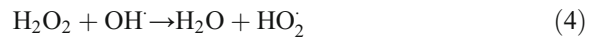
Besides, hydrogen peroxide could also compete with organic matter for the absorption sites on the photocatalyst surface.
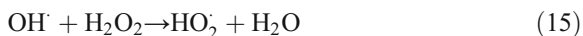
On the other hand, presence of persulfate ions in the solution could increase the photocatalytic degradation rates avoiding recombination of e^-_{CB}/h^+, leaving a larger number of holes able to produce $OH^.$. Reactions for photocatalytic oxidation adding sodium persulfate as oxidant are expressed in Eqs. 5–8 (Pérez et al. 2006).

$$S_2O_8^{2-} + e^-_{CB} \rightarrow SO_4^{2-} + SO_4^{.-} \tag{5}$$

$$SO_4^{.-} + e^-_{CB} \rightarrow SO_4^{2-} \tag{6}$$

$$SO_4^{.-} + H_2O \leftrightarrow SO_4^{2-} + \text{oxidized species} \tag{7}$$

$$S_2O_8^{2-} + hv \rightarrow 2SO_4^{.-} \tag{8}$$

Additionally, $SO_4^{.-}$ radicals are generated through persulfate UV radiation, and they could contribute to organic pollutant removal.

For its part, reactions for Fenton processes are shown in Eqs. 9–15, and for Fenton-like reactions in Eqs. 10 to 15 (Wu et al. 2012).

$$Fe^{2+} + H_2O_2 \rightarrow Fe^{3+} + OH^. + OH^- \tag{9}$$

$$Fe^{3+} + H_2O_2 \rightarrow Fe^{2+} + HO_2^. + H^+ \tag{10}$$

$$Fe^{3+} + H_2O_2 \rightarrow Fe-O_2H^{2+} + H^+ \tag{11}$$

$$Fe-O_2H^{2+} \rightarrow Fe^{2+} + HO_2^. \tag{12}$$

$$Fe^{3+} + H_2O \rightarrow FeOH^{2+} + H^+ \tag{13}$$

$$Fe^{2+} + HO_2^. \rightarrow Fe^{3+} + HO_2^- \tag{14}$$

$$OH^{\cdot} + H_2O_2 \rightarrow HO_2^{\cdot} + H_2O \qquad (15)$$

$$2OH^{\cdot} \rightarrow H_2O_2 \qquad (16)$$

Additionally, in photo-Fenton and photo-Fenton-like processes, additional reactions take place,

$$Fe-O_2H^{2+} + h\nu \rightarrow Fe^{2+} + OH^{\cdot} \qquad (17)$$

$$H_2O_2 + h\nu \rightarrow 2OH^{\cdot} \qquad (18)$$
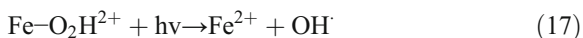
Taking into account the above, in this study, ALC degradation using TiO_2 heterogeneous photocatalysis including the effect of oxidizing agents H_2O_2 and $Na_2S_2O_8$ was analyzed. In addition, pollutant removal under Fenton and photo-Fenton reactions was carried out, and the results were compared. Extent of organic carbon mineralization, ion generation rate, and sample toxicity reduction were also assessed.

2 Materials and Methods

2.1 Chemicals

Aqueous solutions were prepared using distilled purified water (conductivity: 90 μS, total organic carbon (TOC) < 0.5 mg L^{-1}). Analytic grade alachlor (purity > 99%) was supplied by Chemservice and used as analytical standard in liquid and gas chromatography and in photochemical experiments. TiO_2 Degussa P25, hydrogen peroxide 30 and 35% (weight/volume) were supplied by Panreac and Protoquímica. Sodium persulfate, iron sulfate heptahydrate, and ferric chloride hexahydrate analytical grade, supplied by Merck, were used as source of sulfate, ferrous, and ferric ions. Solution pH was adjusted with analytical grade sulfuric acid supplied by Merck.

2.2 Photochemical System

TiO_2 photocatalysis, photo-Fenton, and photo-Fenton-like experiments were carried out in a tubular photo-reactor consisting of a quartz tube equipped with a concentric low pressure mercury lamp (Atlantic Ultraviolet, model MP36B, 38 W), which emits UV monochromatic radiation at 254 nm at a maximum power of 38 W. Reactor dimensions are 86 cm long and 1.5 cm diameter. Alachlor solution flowed through the space between quartz tube and an outer tube made of stainless steel. This reactor is connected to an acrylic circulation tank which has a submergible pump and stirring system for supplying oxygen to the solution. Figure 1 corresponds to a schematic representation of the used dispositive.

ALC initial concentration in the experiments was 50 mg L^{-1} (185.4 μmol L^{-1}). Tests were carried out at 25 °C. Solution was recirculated at a rate of 300 mL min^{-1}, until homogenization was achieved. The volume of solution in the photo-reactor was 10 L. The monitoring time for photolysis and photocatalysis started when the system was completely filled and mixed. Hydrolysis assays were made in three flasks filled with 500 mL of pesticide solution. pH was adjusted to 2.7, 7, and 9, and solutions were left in the dark for 5 days.

For photocatalysis tests, solution at desired initial concentration was transferred to the reactor. Mix was recycled through the system during 15 min to achieve homogenization. After homogenization, the lamp was turned on and samples were taken every 5 min at the beginning of irradiation, and subsequently every 10 min. No pH adjustment was made during the photo-degradation tests. Additional experiments at 50 mg L^{-1} of TiO_2 in the presence of hydrogen peroxide (H_2O_2) at initial concentrations of 250, 500, and 750 mg L^{-1}, and of sodium persulfate ($Na_2S_2O_8$) at initial concentrations of 595, 1190, and 2381 mg L^{-1} were carried out.

In photo-Fenton and photo-Fenton-like processes, pH for all samples was adjusted to 2.8. Subsequently, iron ions were added as ferrous sulfate heptahydrate ($FeSO_4 \cdot 7H_2O$) at concentrations of 2, 10, and 56 mg L^{-1} and recirculated every 15 min. H_2O_2 was added in a concentration of 500 mg L^{-1} and recirculated for 15 min. H_2O_2 was dosed during the experiment in order to obtain a concentration in excess during all the test. An additional Fenton-like test was made adding ferric chloride hexahydrate ($FeCl_3 \cdot 6H_2O$) at a concentration of Fe^{+3} of 10 mg L^{-1}.

2.3 Analytical Methods

For monitoring the concentration of alachlor, an HPLC system (Agilent Technologies 1100 Series) was used. It consists of a high pressure pump for four solvents, a diode array detector, and a system with sample injection

Fig. 1 Schematic representation
of the photo-reactor
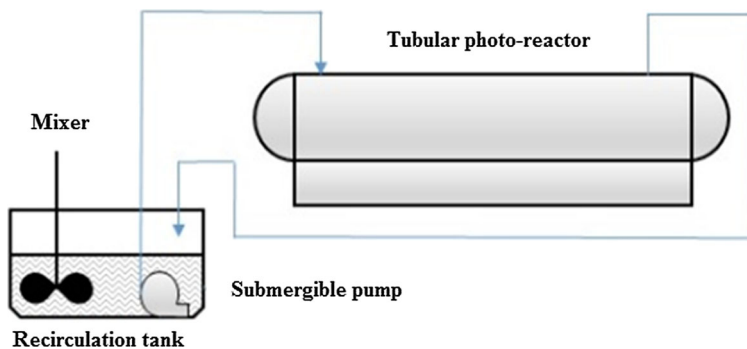
valve, a 20-μm injection loop, and a thermostat column oven. The pesticide was analyzed using a C18 column (Merck, 125 mm × 4 mm; 5 μm). The wavelength for detection was 210 nm. Column temperature was 25 °C and injection volume was 10 μL. Eluent was ultrapure water/acetonitrile at a ratio of 40/60 and a flow rate of 1.0 mL min^{-1}. Under these conditions, alachlor detection limit was 0.0047 mg L^{-1} and quantification limit was 0.1 mg L^{-1}.

Degradation by-products were identified using a gas chromatograph (Agilent model 7890A) with autosampler coupled to a spectrometer 5975C. A column HP-5MS (30 m × 0.25 mm × 0.25 mm) and helium as carrier gas were used. Injector temperature was 250 °C, detector temperature 270 °C, and an oven temperature ramp from 100 to 210 °C at a rate of 15 °C min^{-1}.

Chloride, nitrite, nitrate, and sulfate ions in solution were analyzed as mineralization products. For this purpose, a DIONEX-120 ion chromatograph, with an IonPac AS14 column (250 mm × 4 mm), an IonPac AG14 precolumn (4 mm), and an ionic conductivity suppressor membrane column ARS-Ultra, was used. The loop injection volume was 100 μL and the flow rate was 1.2 mL min^{-1}. This device was connected to an electronic integrator (Hewlett Packard 3396 series II). The mobile phase was a solution of Na_2CO_3 3.5 mM and $NaHCO_3$ 1 mM.

Total organic carbon was evaluated with a TOC 1010 Analytical IO Total Organic Carbon Analyzer. TOC was determined by differences between total carbon (TC) and inorganic carbon (IC) contents.

H_2O_2 consumption was analyzed adding KI in excess to samples in acid medium for photo-Fenton and photocatalytic treatments assisted by H_2O_2. Starch was then added, and then, titration was made using a standard solution of sodium or potassium thiosulfate.

$Na_2S_2O_8$ concentration was measured by precipitating the sulfate ion in acetic acid in presence of barium chloride.

Potentiometric determination of nitrates was made with an electrode of liquid ion exchange membranes, chlorides with a potentiometric titration system with a silver nitrate solution 0.0141 N in a system with glass electrode, and silver/silver chloride. Ammonia nitrogen and total nitrogen were also analyzed by the Kjeldahl method.

Finally, a potassium ferroxioxalate actinometer was used to determine the radiation intensity of the mercury lamp, via oxidation of oxalate $K_3Fe(C_2O_4)_3 \cdot H_2O$, or reduction of Fe^{+3} based on the method described by Hatchard and Parker (1956).

2.4 Toxicity Analysis

Toxicity studies were performed with *Daphnia pulex* crustacean. It was acclimated to 21 ± 1 °C over a period of 16 h light and 8 of darkness and illumination of 1000 to 1500 lx, with dissolved oxygen above 60% saturation. They were fed daily with a mixture of alfalfa plus TetraMin. The specimens for toxicity test were fed 2 h before testing. Two hundred neonates were exposed for toxicity testing, with 10 individuals per test. Dilutions of samples from degradation treatments were prepared, 10 neonates transferred to each vessel for a period of 48 h. After incubation, test vessels were revised and the number of dead organisms (motionless) verified.

3 Results and Discussion

3.1 Hydrolysis Experiments

Control experiments with solutions of 50-mg L^{-1} alachlor initial concentration in the dark at pH 2.7, 7, and 9

(data not shown) indicated that hydrolysis in 5 days was negligible regardless of pH. This stability for alachlor in aqueous solution in the absence of light has been previously reported by Chu and Wong (2004) and Lizama and Silva (2006) (Lizama and Silva 2006; Chu and Wong 2004).

3.2 Photolysis Experiments

Photolysis results (data not shown) indicate that alachlor in aqueous solutions (initial concentration 50 mg L^{-1}) could be completely degraded within 5 h of radiation (UV 254 nm) and a TOC reduction of 10%. These results are similar to those reported by other authors (Huang et al. 2017; Katsumata et al. 2006; Wong and Chu 2003). However, it is important to highlight that the low TOC reduction implies that some of the photo-generated by-products are recalcitrant and it is necessary to use other kind of treatment technologies in order to guarantee its removal from water bodies, in special because some of them could have more toxicity than ALC.

3.3 ALC Removal Using TiO_2 Heterogeneous Photocatalysis

Results of ALC removal employing TiO_2 photocatalysis are showed in Fig. 2. In this way, it can be seen that pollutant was removed totally in less than 80 min of photo-treatment, and a complete mineralization of the organic matter content in the solution was reached in around 400 min. In addition, Fig. 3 shows the influence of initial concentration of alachlor on degradation times. Effect of ALC initial concentration on process was evaluated considering values of 10, 25, 50, 83, and 124 mg L^{-1} obtaining total degradation times of less than 30, 50, 80, 90, and 120 min, respectively.

Initial degradation rates (r_0) and time necessary to achieve 90% mineralization ($t_{90\%,TOC}$) are presented in Table 1. From the table, it can be noted that as ALC initial concentration increases, initial degradation rate increases, but also does degradation and mineralization time.

3.4 ALC Removal Using TiO_2 Heterogeneous Photocatalysis Under the Presence of H_2O_2 and $Na_2S_2O_8$

Figure 4 shows the results for alachlor mineralization using TiO_2 heterogeneous photocatalysis under the presence of H_2O_2.

According to Fig. 4 and Eqs. 3 and 4, addition of H_2O_2 into the solution has a positive effect on organic matter mineralization. However, if peroxide presence is very high, it acts as a radical scavenger and pollutant removal and mineralization are diminished. In this way, under the evaluated experimental conditions, the optimized H_2O_2/alachlor molar ratio corresponds to around 79 (500 mg L^{-1} H_2O_2/50 mg L^{-1} ALC), with a mineralization rate constant of 0.015 min^{-1}, and mineralization time of around 300 min, shorter than that obtained using the conventional TiO_2 heterogeneous photocatalysis. These results are consistent with those reported by other researches, who indicated that the optimal molar ratios for similar removal of similar organic compounds using H_2O_2/TiO_2 photocatalysis are between 10 and 100 (Malato et al. 2000).

On the other hand, Fig. 5 shows the results obtained for alachlor mineralization using TiO_2 photocatalysis under the presence of sodium persulfate. From the figure, it can be seen that increments on $S_2O_8^{2-}$ presence in the solution contribute to organic matter oxidation. In particular, under 2380 mg L^{-1} concentration of that ion, total mineralization time was at least seven times shorter than the necessary under the treatment using only TiO_2 and UV radiation. These results are consistent with the information presented by Eqs. 5–8, in which the positive effect of persulfate ions on organic pollutant removal is indicated.

3.5 ALC Removal Using Fenton and Photo-Fenton Technologies

Figure 6 shows the results about the alachlor degradation and mineralization using Fenton and photo-Fenton technologies under Fe^{+2} initial concentrations of 2.0, 10.0, and 56.0 mg L^{-1} and a H_2O_2 concentration of 500 mg L^{-1}. Results indicated that pollutant concentration was significantly reduced during Fenton reaction in the dark for all the Fe^{+2}-evaluated concentrations, being the most efficient 56 mg L^{-1}. At this ferrous ion concentration, ALC was completely removed in less than 60 min without UV light irradiation, and total organic matter mineralization was reached after 120 min of irradiation. This aspect indicated that Fenton technology is able to remove ALC from aqueous matrices, but it is necessary to implement other kind of methodologies to get a total oxidation or the organic matter present in the evaluated samples.
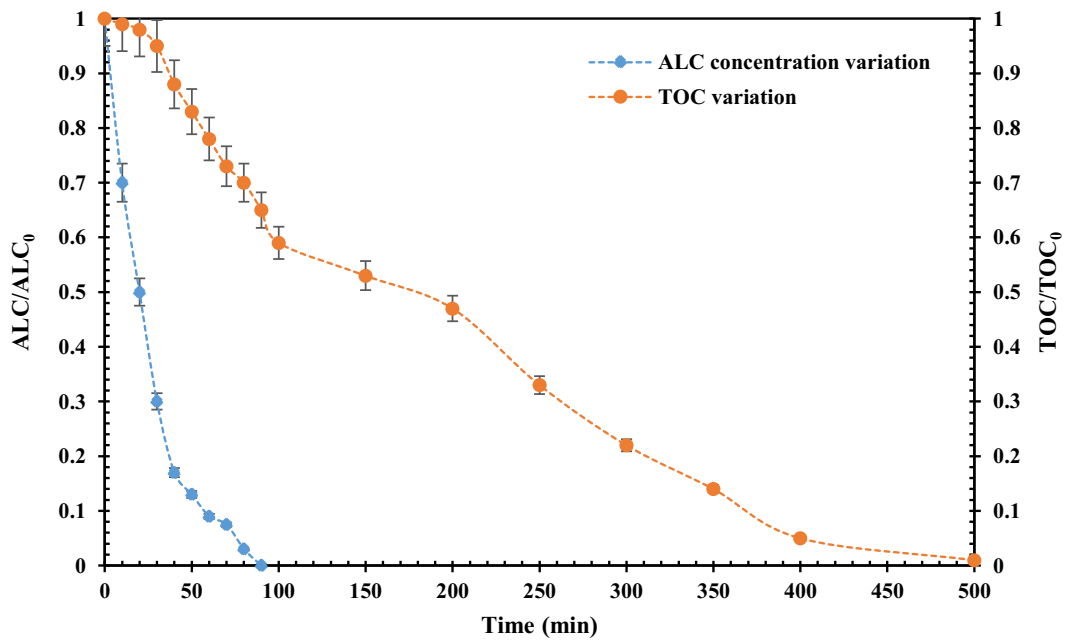
Fig. 2 ALC removal using TiO$_2$ heterogeneous photocatalysis (pollutant initial concentration: 50.0 mg L^{-1}, catalyst initial concentration: 50.0 mg L^{-1}, average temperature: 25 ± 2 °C, pH: 7.0)

Effectiveness on mineralization for photo-Fenton processes can be explained by reaction 17, in which radical Fe^{2+} is regenerated producing additional OH$^-$ radicals as consequence of the effect of UV light radiation. Besides, under UV radiation, H$_2$O$_2$ could generate additional hydroxyl radicals that would be available for organic compound elimination. In this way, photo-Fenton process would represent a more
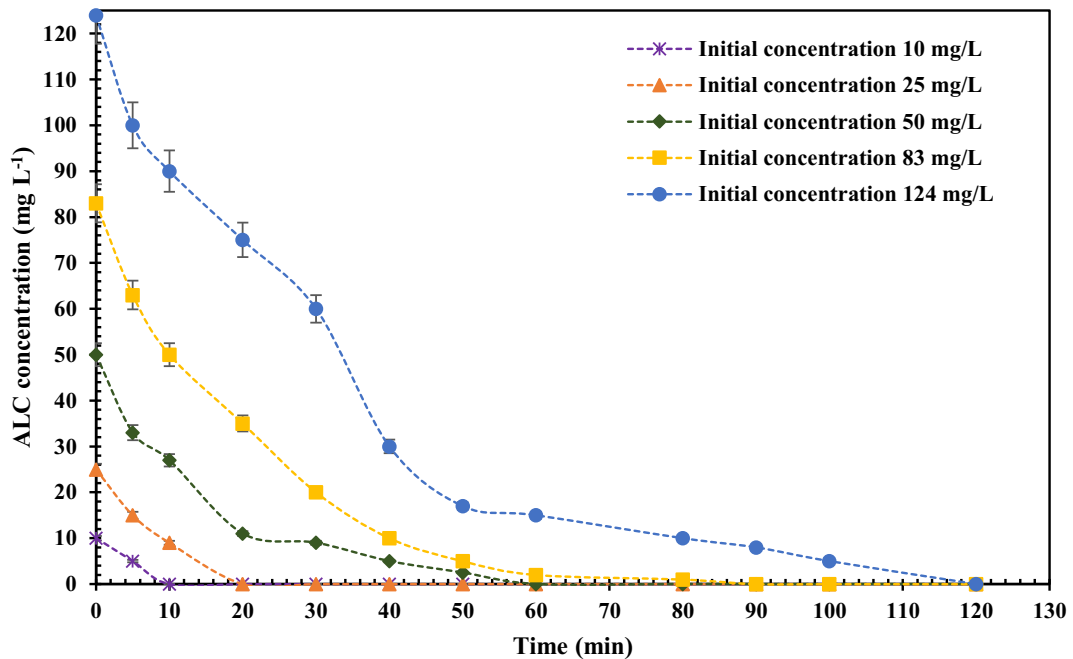

Fig. 3 Effect of pollutant initial concentration on ALC removal using TiO$_2$ heterogeneous photocatalysis (catalyst initial concentration: 50.0 mg L^{-1}, average temperature: 25 ± 2 °C, pH: 7.0)

Table 1 Time for 90% mineralization and initial alachlor degradation rates by photocatalysis (catalyst initial concentration: 50.0 mg L^{-1}, average temperature: 25 ± 2 °C, pH: 7.0)

Alachlor initial concentration							
10 mg L^{-1}		25 mg L^{-1}		50 mg L^{-1}		124 mg L^{-1}	
$t_{90\%, TOC}$ (min)	r_0 (mg L^{-1} min^{-1})	$t_{90\%, TOC}$ (min)	r_0 (mg L^{-1} min^{-1})	$t_{90\%, TOC}$ (min)	r_0 (mg L^{-1} min^{-1})	$t_{90\%, TOC}$ (min)	r_0 (mg L^{-1} min^{-1})
105	0.802	152	0.846	300	1.26	900	1.92

efficient way to achieve total pollutant mineralization, and implementation implies less H_2O_2 requirements and a faster ferrous ion regeneration.

On the other hand, the use of ferric salts for ALC degradation using Fenton technologies could represent an advantageous option in an economic point of view since they are cheaper than ferrous salts. However, Fe^{+3} ions react much slower with H_2O_2 than Fe^{+2} ions; hence, regeneration of Fe^{+2} (Eq. 12) is usually the limiting step of most Fenton and Fenton-like systems. In this way, in order to find out the effect of ferric ions in alachlor degradation, an experiment using a Fe^{+3} concentration of 10 mg L^{-1} at the same H_2O_2 concentration used in previous experiments with Fe^{+2} was carried out. Fe^{+3} source was ferric chloride. Figure 7 shows the obtained results and the pollutant removal under both photo-treatments.

From Fig. 7, it can be seen that without UV radiation, ALC removal with Fe^{2+} is faster than with Fe^{+3}, a fact that could be explained by the slower reaction rate of Fe^{+3} ions with H_2O_2, but also by the OH^- radicals scavenging by Cl^- ions from the ferric salt. The reaction of OH^- with Cl^- leads to the formation of chlorine atoms (Cl^-) and dichloride anion radicals (Cl^-_2). These two species are strong oxidizing agents, being able to oxidize H_2O_2 and Fe^{2+}, but are less reactive with organic solutes than OH^- radicals (Pérez et al. 2006). In addition, chloride ion presence may have negative effects on the efficiency of the Fe^{+2}/H_2O_2 and Fe^{+3}/H_2O_2 systems as result of the formation of Fe^{+3} chlorocomplexes (Cui et al. 2015). However, once UV irradiation started, degradation rates for Fe^{+2} and Fe^{+3} systems were very similar. Then, it could be concluded that despite the negative effects of the Fe^{+3}
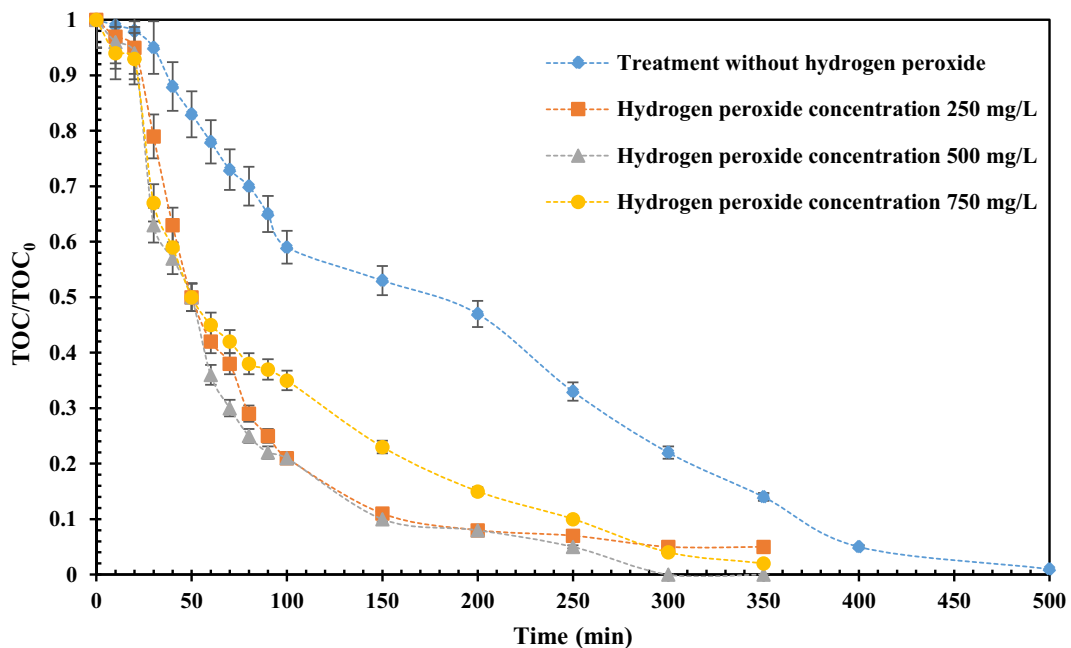
Fig. 4 Effect of H_2O_2 presence on ALC removal using TiO_2 heterogeneous photocatalysis (pollutant initial concentration: 50.0 mg L^{-1}, catalyst initial concentration: 50.0 mg L^{-1}, average temperature: 25 ± 2 °C, pH: 7.0)
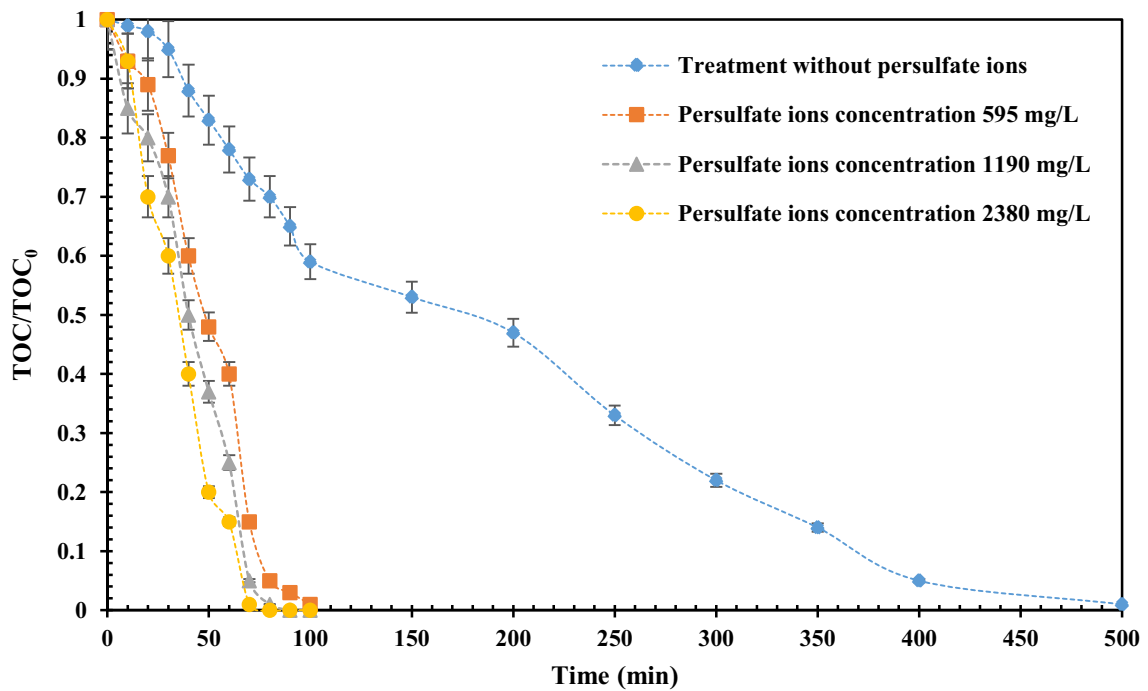
Fig. 5 Effect of $S_2O_8^{2-}$ ion presence on ALC removal using TiO_2 heterogeneous photocatalysis (pollutant initial concentration: 50.0 mg L^{-1}, catalyst initial concentration: 50.0 mg L^{-1}, average temperature: 25 ± 2 °C, pH: 7.0)

and chloride ions in the system, FeCl$_3$ would be a good ferric ion source to ALC removal using photo-Fenton-like processes.

Finally, Fig. 8 presents a comparison of pollutant and mineralization variation profiles using photocatalysis with 50 mg L^{-1} of TiO_2, photocatalysis assisted by
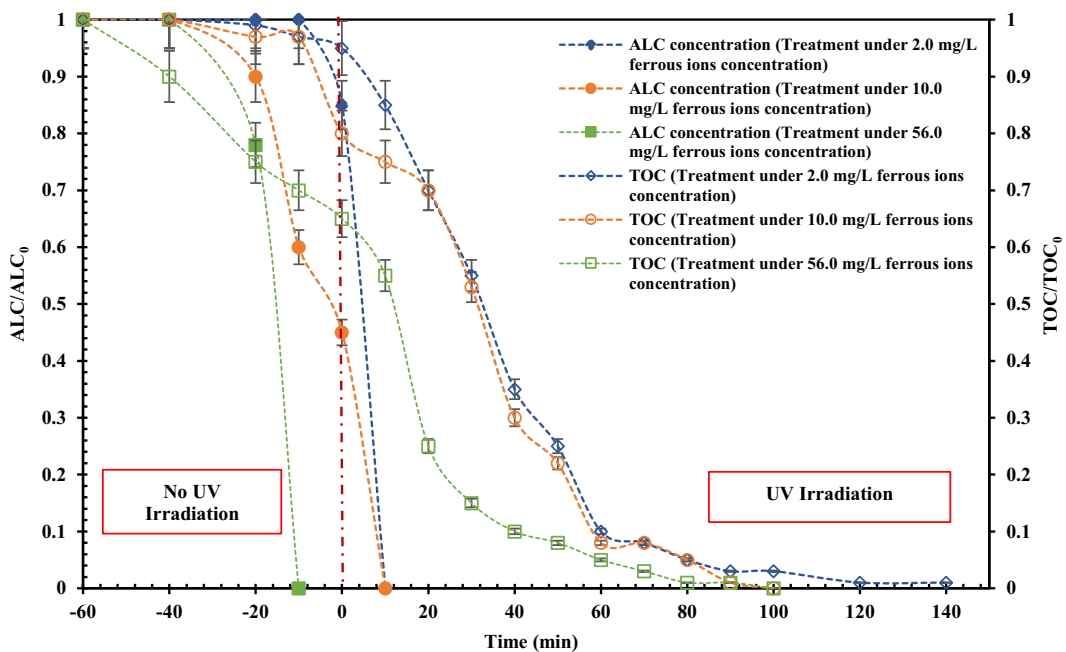

Fig. 6 ALC removal using Fenton and photo-Fenton (pollutant initial concentration: 50.0 mg L^{-1}, H$_2$O$_2$ concentration: 500.0 mg L^{-1}, average temperature: 25 ± 2 °C, pH: 3.0)
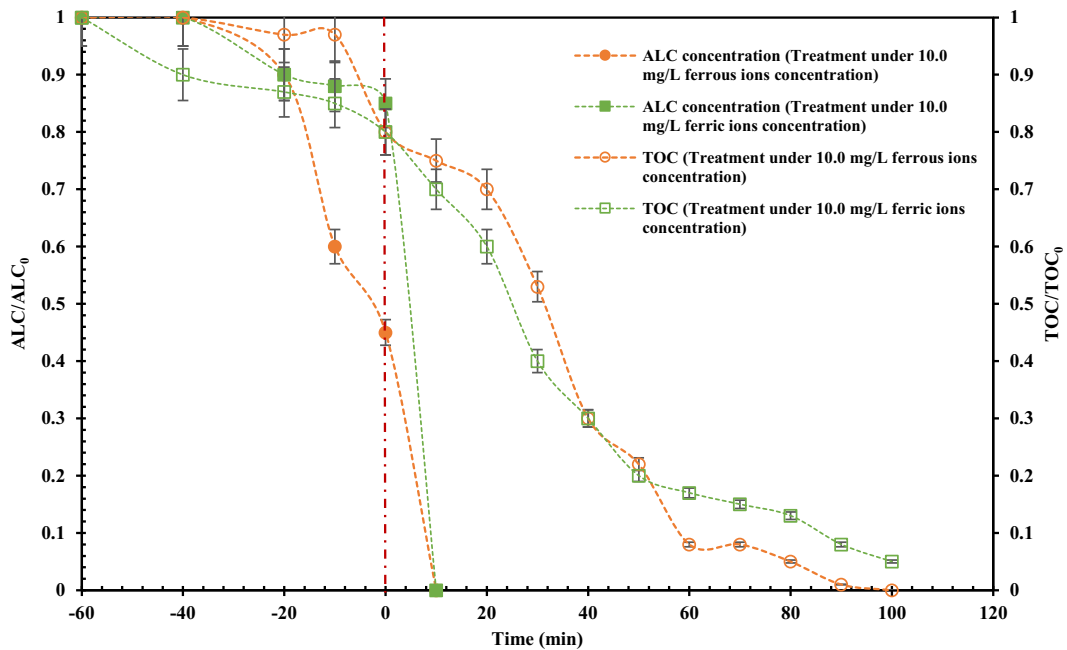
Fig. 7 ALC removal using ferric and ferrous ions in Fenton/photo-Fenton reactions (pollutant initial concentration: 50.0 mg L^{-1}, H$_2$O$_2$ concentration: 500.0 mg L^{-1}, average temperature: 25 ± 2 °C, pH: 3.0)

H$_2$O$_2$ (500 mg L^{-1}) and Na$_2$S$_2$O$_8$ (2381 mg L^{-1}), and photo-Fenton with 56 mg L^{-1} of Fe^{+2} and 500 mg L^{-1} of H$_2$O$_2$.

Times for alachlor total removal and mineralization followed the order photo-Fenton < photocatalysis with persulfate < photo-Fenton-like < photocatalysis with hydrogen peroxide < photocatalysis with TiO$_2$. In this sense, organic matter mineralization under photo-Fenton process was around six times faster than using heterogeneous photocatalysis with TiO$_2$.
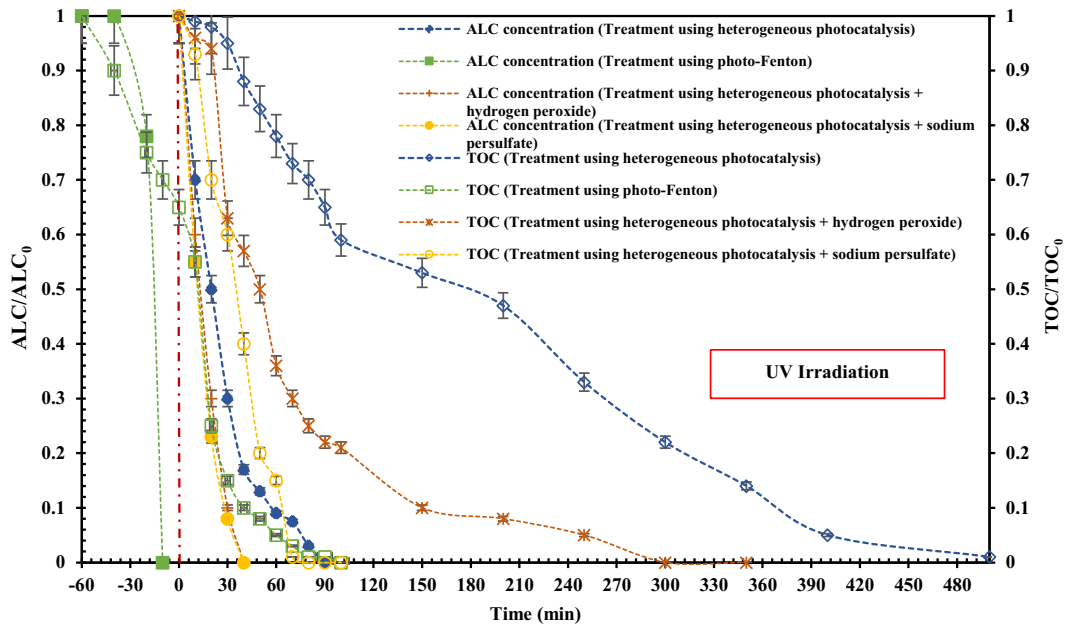

Fig. 8 ALC removal using heterogeneous photocatalysis and photo-Fenton technologies (pollutant initial concentration: 50.0 mg L^{-1}, average temperature: 25 ± 2 °C)
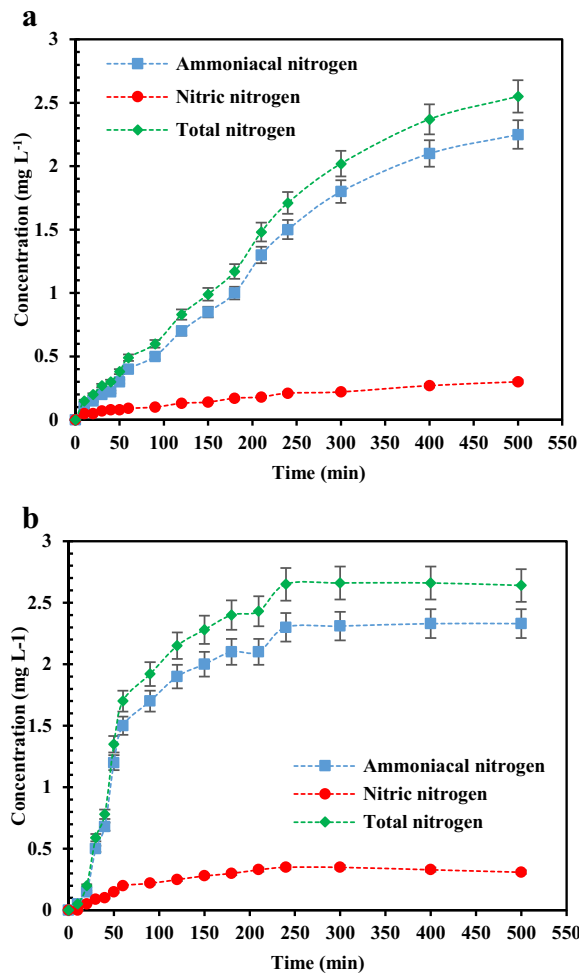
Fig. 9 Nitrogen presence in treated solutions using **a** heterogeneous photocatalysis and **b** photo-Fenton technologies (pollutant initial concentration: 50.0 mg L^{-1}, average temperature: 25 ± 2 °C)

3.6 Inorganic Ion Evaluation

In addition to sample TOC evolution, it might be of interest to compare inorganic release of heteroatoms, such as chlorine, ammonia, and/or nitrate. When total mineralization of alachlor is achieved, nitrogen could be released into the solution as a combination of ammonium and nitrate, but under a sufficient reaction time, ammonium could be totally oxidized to nitrate. In this way, Fig. 9 presents the ammoniacal and nitric nitrogen concentration evolution during sample treatment using heterogeneous photocatalysis and photo-Fenton. From results, it can be noted that at 400 min of photo-treatments, 100% conversion (stoichiometrically) of the alachlor nitrogen content was achieved. Besides, most of the N content in the solutions was in form of ammonia

indicating that NO_3^- is susceptible to oxidation inside the reactive medium.

On the other hand, Fig. 10 allows to observe that chloride ion concentration in samples was quickly increased with increasing the reaction time, a situation that indicates that degradation/dechlorination stage occurs very fast during the pollutant photo-treatment. The total amount of chloride ion produced after 120 min of reaction was approximately 6.60 mg L^{-1} corresponding to a 100% conversion of the alachlor chloride content.

3.7 By-product Identification

Degradation by-products for ALC photocatalytic treatment were studied using a GC-MS mass spectrometer. In this way, hydroxyalachlor, N-(2,6-diethylphenyl) methylamine, and lactam (8-ethyl-methoxymethyl-4-methyl-2-oxo-1,2,3,4,tetraquinoline) were identified. In general, different authors have reported that pollutant removal under advanced oxidation processes proceeds via homolytic breakage of the C–Cl bond, followed by co-entrapment of radical co-formed by water or by an intramolecular hydrogen abstraction (Hapeman-Somich 1991; Kumar et al. 2017; Pérez et al. 2006). Finally, the results found in this study support that degradation of alachlor by photocatalysis with TiO$_2$ comes from bond breaking or by oxidation of the N-methoxy methyl group and a subsequent mineralization of the organic matter. Table 2 presents the molecular structures, main fragments, and retention times from ALC and the identified by-products.
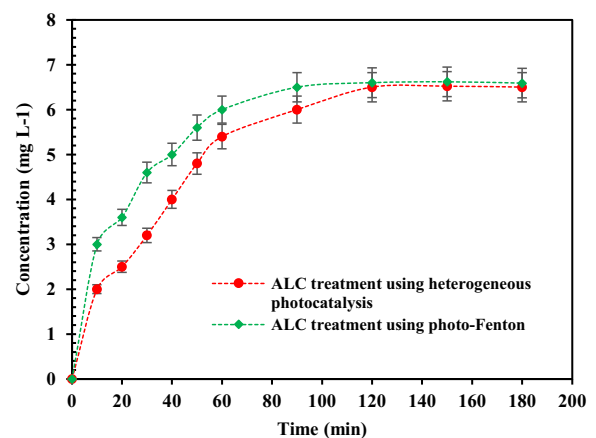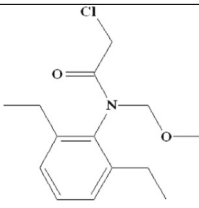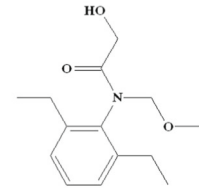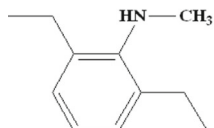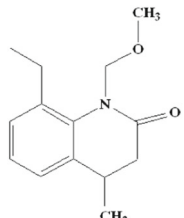

Fig. 10 Chloride ion presence in treated solutions using heterogeneous photocatalysis and photo-Fenton technologies for ALC removal (pollutant initial concentration: 50.0 mg L^{-1}, average temperature: 25 ± 2 °C)

Table 2 Identified intermediates during photocatalytic degradation of ALC

Compound	Molecular structure	Main fragments (m/z)	Retention time (min)
Alachlor		162, 148, 45	9.83
Hydroxyalachlor		188, 45, 28	9.23
N- (2,6-diethylphenyl) methylamine		163, 148, 28	6.18
Lactam (8-ethyl-methoxymethyl-4-methyl-2-oxo-1,2,3,4,tetraquinoline)		186, 46, 28	8.76

3.8 Toxicity Studies

Figure 11 shows the evolution of toxicity assays (expressed in mortality percentage) using *Daphnia pulex* crustacean during sample treatment under
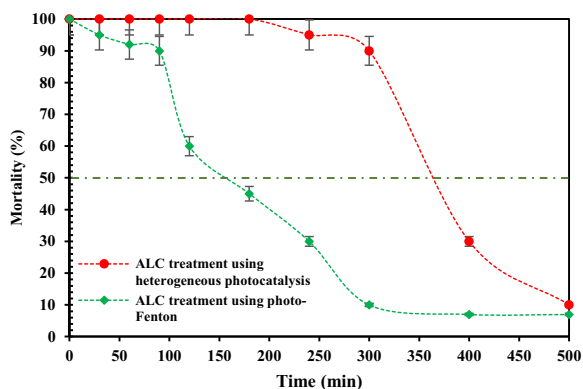

Fig. 11 Toxicity evolution using heterogeneous photocatalysis and photo-Fenton technologies for ALC removal (pollutant initial concentration: 50.0 mg L^{-1}, average temperature: 25 ± 2 °C)

heterogeneous photocatalysis with TiO$_2$ and photo-Fenton processes. From results, it can be inferred that during the photocatalysis process, a 50% mortality reduction was achieved after 450 min of treatment while during the photo-Fenton process, this reduction was reached after 180 min, demonstrating that photo-Fenton technology is faster for toxicity decreasing.

4 Conclusions

It was demonstrated that TiO$_2$ heterogeneous photocatalysis and photo-Fenton processes with UV radiation at 254 nm are useful treatments for water contaminated with alachlor. Additionally, pollutant removal was faster using Fenton reaction than under the photocatalytic process with TiO$_2$, even if oxidizing agents such as H$_2$O$_2$ and Na$_2$S$_2$O$_8$ are added.

Fenton process was sufficient for a total alachlor degradation, but not for total mineralization, that was

reached under irradiation conditions in all the evaluated systems. Without UV radiation, pollutant oxidation with Fe^{2+} was faster than oxidation with Fe^{3+}, but once irradiation started, degradation rates were very similar, showing that $FeCl_3$ could be a good ferric ion source to degrade alachlor under Fenton and photo-Fenton-like technologies.

References

Chu, W., & Wong, C. C. (2004). Study of herbicide alachlor removal in a photocatalytic process through the examination of the reaction mechanism. *Industrial and Engineering Chemistry Research, 43*(17), 5027–5031. https://doi.org/10.1021/ie0342356.

Cui, L., Cheng, F., & Zhou, J. (2015). Behaviors and mechanism of Iron extraction from chloride solutions using undiluted Cyphos IL 101. *Industrial and Engineering Chemistry Research, 54*(30), 7534–7542. https://doi.org/10.1021/acs.iecr.5b01546.

Directive 2000/7/EC. (2000). Directive 2000/60/EC of the European Parliament and of the council of 23 October 2000 establishing a framework for community action in the field of water policy. *Official Journal of the European Parliament, L327*(September 1996), 1–82. https://doi.org/10.1039/ap9842100196.

Hapeman-Somich, C. J. (1991). Mineralization of pesticide degradation products. In *Pesticide Transformation Products: Fate and Significance in the Environment, ACS Symposium Series, 1991* (pp. 133–147). https://doi.org/10.1021/bk-1991-0459.ch010.

Hatchard, C. G., & Parker, C. A. (1956). A new sensitive chemical Actinometer. II. Potassium Ferrioxalate as a standard chemical Actinometer. *Proceedings of the Royal Society A: Mathematical, Physical and Engineering Sciences, 235*(1203), 518–536. https://doi.org/10.1098/rspa.1956.0102.

Huang, X., Hou, X., Jia, F., Song, F., Zhao, J., & Zhang, L. (2017). Ascorbate-promoted surface Iron cycle for efficient heterogeneous Fenton Alachlor degradation with hematite nanocrystals. *ACS Applied Materials and Interfaces, 9*(10), 8751–8758. https://doi.org/10.1021/acsami.6b16600.

Katsumata, H., Kaneco, S., Suzuki, T., Ohta, K., & Yobiko, Y. (2006). Photo-Fenton degradation of alachlor in the presence of citrate solution. *Journal of Photochemistry and Photobiology A: Chemistry, 180*(1–2), 38–45. https://doi.org/10.1016/j.jphotochem.2005.09.013.

Kumar, Y. B., Singh, N., & Singh, S. B. (2017). Removal of herbicides mixture of atrazine, metribuzin, metolachlor and

alachlor from water using granular carbon. *Indian Journal of Chemical Technology, 24*(4), 400–404. https://doi.org/10.4172/2161-0525.1000196.

de Luna, M. D. G., Rivera, K. K. P., Suwannaruang, T., & Wantala, K. (2015). Alachlor photocatalytic degradation over uncalcined Fe–TiO2 loaded on granular activated carbon under UV and visible light irradiation. *Desalination and Water Treatment, 57*(15), 1–11. https://doi.org/10.1080/19443994.2015.1011706.

Lizama, C., & Silva, S. (2006). Photodegradation of chlorbromuron, atrazine, and alachlor in aqueous systems under solar irradiation. *International Journal of Photoenergy, 2006*, 1–6. https://doi.org/10.1155/IJP/2006/81808 .

Malato, S., Blanco, J., Maldonado, M. I., Fernández-Ibáñez, P., & Campos, A. (2000). Optimising solar photocatalytic mineralisation of pesticides by adding inorganic oxidising species; application to the recycling of pesticide containers. *Applied Catalysis B: Environmental, 28*(3–4), 163–174. https://doi.org/10.1016/S0926-3373(00)00175-2.

Pérez, M. H., Peñuela, G., Maldonado, M. I., Malato, O., Fernández-Ibáñez, P., Oller, I., et al. (2006). Degradation of pesticides in water using solar advanced oxidation processes. *Applied Catalysis B: Environmental, 64*(3–4), 272–281. https://doi.org/10.1016/j.apcatb.2005.11.013.

Pichat, P., Guillard, C., Amalric, L., Renard, A.-C., & Plaidy, O. (1995). Assessment of the importance of the role of H_2O_2 and $O_2^{\cdot-}$ in the photocatalytic degradation of 1,2-dimethoxybenzene. *Solar Energy Materials and Solar Cells, 38*(1–4), 391–399. https://doi.org/10.1016/0927-0248(94)00231-2 .

Potter, T., & Carpenter, T. (1995). Occurrence of Alachlor environmental degradation products in groundwater. *Science, 29*(6), 1557–1563. https://doi.org/10.1021/es00006a018.

Ritter, W. F. (1990). Pesticide contamination of ground water in the United States - a review. *Journal of Environmental Science and Health, Part B, 25* (1), 1–29. https://doi.org/10.1080/03601239009372674.

United States Environmental Protection Agency (EPA) 2009. National Primary Drinking Water Regulations. Ground Water and Drinking Water. https://www.epa.gov/ground-water-and-drinking-water/national-primary-drinking-water-regulations. Accessed 20 June 2018.

Wang, Q., Shao, Y., Gao, N., Chu, W., Deng, J., Shen, X., et al. (2016). Degradation of alachlor with zero-valent iron activating persulfate oxidation. *Journal of the Taiwan Institute of Chemical Engineers, 63*, 379–385. https://doi.org/10.1016/j.jtice.2016.03.038.

Wong, C. C., & Chu, W. (2003). The hydrogen peroxide-assisted photocatalytic degradation of alachlor in TiO2 suspensions. *Environmental Science and Technology, 37*(10), 2310–2316. https://doi.org/10.1021/es020898n .

Wu, C. H., Andy Hong, P. K., & Jian, M. Y. (2012). Decolorization of reactive red 2 in Fenton and Fenton-like systems: Effects of ultrasound and ultraviolet irradiation. *Reaction Kinetics, Mechanisms and Catalysis, 106*(1), 11–24. https://doi.org/10.1007/s11144-012-0420-x.